Denote $\bar{\Omega} = 1 - \Omega$, we express $\bar{\Omega}$ as follows:

$$\bar{\Omega} = E_{\Phi_\ell}\left\{\prod_{\ell\in\Phi_\ell} F_{|\hat{g}_\ell|^2}\left(\frac{(1+d_\ell^\alpha)\,\rho_p}{x}\right)\right\}. \tag{A.2}$$

Applying the generating function, we rewrite (A.2) as follows:

$$\bar{\Omega} = \exp\left[-\lambda_\ell \int\limits_{R^2} \left(1 - F_{|\hat{g}_\ell|^2}\left((1+d_\ell^\alpha)\,\mu\right)\right) r dr\right] = \exp\left[-2\pi\lambda_\ell e^{-\mu} \int\limits_0^\infty r e^{-\mu r^\alpha} dr\right]. \tag{A.3}$$

Applying [14, eq. (3.326.2)], we obtain

$$\Omega = 1 - \bar{\Omega} = 1 - e^{-\frac{e^{-\mu}\delta\pi\lambda_\ell\Gamma(\delta)}{\mu^\delta}} \tag{A.4}$$

where $\Gamma(\cdot)$ is the Gamma function. Substituting (A.4) into (A.1) and taking the derivative, we obtain the pdf of γ_t in (16). The proof is completed.

References

[1] Y. Saito, A. Benjebbour, Y. Kishiyama, and T. Nakamura, "System-level performance evaluation of downlink non-orthogonal multiple access (NOMA)," in *Proc. IEEE Annu. Symp. PIMRC*, Sep. 2013, pp. 611–615.

[2] Z. Ding, Z. Yang, P. Fan, and H. V. Poor, "On the performance of non-orthogonal multiple access in 5G systems with randomly deployed users," *IEEE Signal Process. Lett.*, vol. 21, no. 12, pp. 1501–1505, Dec. 2014.

[3] M. Al-Imari, P. Xiao, M. A. Imran, and R. Tafazolli, "Uplink non-orthogonal multiple access for 5G wireless networks," in *Proc. IEEE 11th ISWCS*, Barcelona, Spain, Aug. 2014, pp. 781–785.

[4] Z. Ding, F. Adachi, and H. V. Poor, "The application of MIMO to non-orthogonal multiple access," *IEEE Trans. Wireless Commun.*, vol. 15, no. 1, pp. 537–552, Jan. 2016.

[5] Q. Sun, S. Han, C.-L. I, and Z. Pan, "On the ergodic capacity of MIMO NOMA systems," *IEEE Wireless Commun. Lett.*, vol. 4, no. 4, pp. 405–408, Aug. 2015.

[6] A. Goldsmith, S. A. Jafar, I. Maric, and S. Srinivasa, "Breaking spectrum gridlock with cognitive radios: An information theoretic perspective," *Proc. IEEE*, vol. 97, no. 5, pp. 894–914, May 2009.

[7] Y. Dhungana and C. Tellambura, "Outage probability of underlay cognitive relay networks with spatially random nodes," in *Proc. GLOBECOM*, Dec. 2014, pp. 3597–3602.

[8] Z. Ding, P. Fan, and H. V. Poor, "Impact of user pairing on 5G non-orthogonal multiple access," *IEEE Trans. Veh. Technol.*, vol. 65, no. 8, pp. 6010–6023, Aug. 2016.

[9] M. Haenggi, *Stochastic Geometry for Wireless Networks*. Cambridge, U.K.: Cambridge Univ. Press, 2012.

[10] J. Venkataraman, M. Haenggi, and O. Collins, "Shot noise models for outage and throughput analyses in wireless ad hoc networks," in *Proc. MILCOM*, 2006, pp. 1–7.

[11] T. M. Cover and J. A. Thomas, *Elements of Information Theory*, 2nd ed. New York, NY, USA: Wiley, 2006.

[12] H. A. David and N. Nagaraja, *Order Statistics*, 3rd ed. New York, NY, USA: Wiley, 2003.

[13] E. Hildebrand, *Introduction to Numerical Analysis*. New York, NY, USA: Dover, 1987.

[14] I. S. Gradshteyn and I. M. Ryzhik, *Table of Integrals, Series and Products*, 6th ed. New York, NY, USA: Academic, 2000.

A Differential ML Combiner for Differential Amplify-and-Forward System in Time-Selective Fading Channels

Yi Lou, Yong-Kui Ma, Qi-Yue Yu, *Member, IEEE*, Hong-Lin Zhao, *Member, IEEE*, and Wei Xiang, *Senior Member, IEEE*

***Abstract*—We propose a new differential maximum-likelihood (DML) combiner for noncoherent detection of the differential amplify-and-forward (D-AF) relaying system in the time-selective channel. The weights are computed based on both the average channel quality and the correlation coefficient of the direct and relay channels. Moreover, we derive a closed-form approximate expression for the average bit error rate (BER), which is applicable to any single-relay D-AF system with fixed weights. Both theoretical and simulated results are presented to show that the time-selective nature of the underlying channels tends to reduce the diversity gains at the low-signal-to-noise-ratio (SNR) region, resulting in an asymptotic BER floor at the high-SNR region. Moreover, the proposed DML combiner is capable of providing significant BER improvements compared with the conventional differential detection (CDD) and selection-combining (SC) schemes.**

***Index Terms*—Amplify and forward (AF), differential modulation, noncoherent detection, performance analysis, time-varying channels.**

I. Introduction

Cooperative communications has received much attention since it is capable of improving system performance and extending coverage. Thus, several relay-assisted architectures have been adopted by the Third Generation Partnership Project Long Term Evolution-Advanced and IEEE 802.16j standards [1]. It is widely anticipated that cooperative communications will act as a key technology for fifth-generation [2]–[4] mobile communications. Amplify and forward (AF) [5] is a viable technique of cooperative communications from the practical point of view because of its simple implementation and security [6].

It is well known that a moving terminal will induce the Doppler shift, which is the cause of the time selectivity in the fast-fading channel. The impact of outdated channel state information (CSI) on the AF relaying system that employs a relay selection scheme is analyzed in [7] and [8]. The same impact analysis is then extended to the turbo coded relay system over the Nakagami-m channel in [9]. In [10], a weighted two-way relay-selection scheme was proposed whereby the weights take into consideration the correlation coefficient of the time-selective channel. In [11], the impact of different CSI estimation rates on the error performance of a multirelay AF system employing maximal ratio that combines over the time-selective fading channel was studied. Then, the same performance analysis was extended to relay selection in the presence of channel estimation errors in [12].

Manuscript received August 17, 2015; revised December 16, 2015; accepted February 21, 2016. Date of publication February 26, 2016; date of current version December 14, 2016. This work was supported in part by the Key Laboratory of Universal Wireless Communications (Beijing University of Posts and Telecommunications), Ministry of Education of China. The review of this paper was coordinated by Prof. J. P. Coon.

Y. Lou, Y.-K. Ma, Q.-Y. Yu, and H.-L. Zhao are with the Department of Communication Engineering, Harbin Institute of Technology, Harbin 150001, China (e-mail: louyi8733@gmail.com; yk_ma@hit.edu.cn; yuqiyue@hit.edu.cn; hitbourne@gmail.com).

W. Xiang is with the College of Science, Technology and Engineering, James Cook University, Cairns, Qld. 4870, Australia (e-mail: wei.xiang@jcu.edu.au).

Color versions of one or more of the figures in this paper are available online at http://ieeexplore.ieee.org.

Digital Object Identifier 10.1109/TVT.2016.2535299

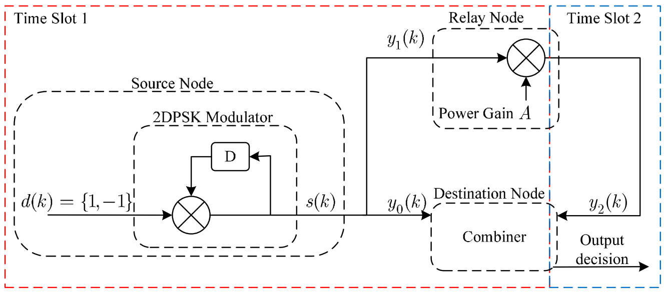

Fig. 1. Block diagram of a three-node D-AF system model.

By adopting differential modulation and noncoherent detection, the differential AF (D-AF) technique can avoid the overhead due to frequent channel estimation at the destination. In [13]–[15], a conventional differential detection (CDD) scheme is proposed to combine the received signals at the destination. The CDD scheme is suitable for only the slow-fading scenario in which the channel gain is assumed unchanged during two consecutive symbol periods. An approximate bit error rate (BER) expression for a single-relay D-AF system employing the selection-combining (SC) scheme in the time-selective channel is derived in [16]. The SC scheme helps lower complexity by eliminating the need for channel estimation at the expense of the BER performance, which is similar to the CDD scheme. Through introducing a modified AR(1) model [17] for the relay link, a diversity combiner, which is called time-varying differential detection (TVD), is proposed in [18] for the D-AF system. A loose lower bound of the BER is also derived by using the instantaneous CSI. However, as the TVD method is proposed for symmetric channels, the impact of the average channel quality on the system performance is not considered. The analysis can be regarded as an extension of the differential scheme with diversity-combining reception for the point-to-point case in [19]–[21].

This paper focuses on the single-relay D-AF system over the time-selective channel. A new differential maximum-likelihood (DML) combiner is proposed that is suitable for a time-selective channel with an arbitrary average channel gain. The weights are computed based on both the second-order statistics and the average channel quality of the involved channels. A novel universal closed-form approximate expression for the average BER is derived for the considered system with a general differential diversity combiner (i.e., with any fixed weights). Based on the average BER, the asymptotic BER limit of the proposed scheme is derived, which is dependent on the autocorrelation of the direct and relay channels. The derived BER expressions are validated through numerical simulations and shown to be very tight under a wide range of fading and average channel gain scenarios.

The rest of this paper is organized as follows. In Section II, the system model is described. The DML combiner is proposed in Section III. Section IV derives the universal closed-form approximate expression for the average BER. Simulation results are presented in Section V. Finally, Section VI concludes this paper.

Notation: $(\cdot)^*$, $|\cdot|$, and $\mathrm{Re}\{\cdot\}$ denote the conjugate, the absolute value, and the real part of a complex variable, respectively. $\mathcal{CN}(0, \sigma^2)$ refers to a complex Gaussian distribution with zero mean and variance σ^2. $E\{\cdot\}$ and $\mathrm{Var}\{\cdot\}$ represent the expectation and variance operations, respectively. $e^{(\cdot)}$ and $E_1(\cdot)$ indicate the exponential function and the exponential integral function, respectively. $O(x)$ is used to represent the high-order terms of x.

II. System and Channel Models

In this paper, a system model similar to that in [16] and [18] is adopted. Fig. 1 illustrates a D-AF system composed of a source S, a semiblind AF relay R, and a destination D. All the nodes are equipped with a single antenna and operate in the half-duplex mode.

Before transmission, the modulated information symbol $d(k)$ drawn from a BPSK constellation $S : \{+1, -1\}$ is encoded differentially as $s(k) = s(k-1)d(k)(s(0) = 1)$. The transmission process takes place in two phases. In the first phase, the source broadcasts $s(k)$ with the average symbol power P_0. The received signals at the destination and relay can be expressed as

$$y_0(k) = \sqrt{P_0}h_0(k)s(k) + n_0(k) \tag{1}$$

$$y_1(k) = \sqrt{P_0}h_1(k)s(k) + n_1(k) \tag{2}$$

where $n_0(k), n_1(k) \sim \mathcal{CN}(0, N_0)$ are the noise components at D and R, respectively.

The received signal at R is then scaled by a power gain A before being forwarded to D in the second phase. The transmissions in two phases are required to be orthogonal to ensure that the received signals at D fade independently. For simplicity, time-division multiple access is adopted. The semiblind power gain is set to $A = \sqrt{P_1/(P_0\sigma_1^2 + N_0)}$ to eliminate the need of frequent channel estimation at R, where P_1 is the average power assigned to the relay. By introducing a power-allocation ratio $\phi \in [0, 1]$, P_0 and P_1 can be related to each other as $P_0 = \phi P$ and $P_1 = (1-\phi)P$, where $P = P_0 + P_1$ is the total transmit power of the system.

For the second time slot, the corresponding received signal $y_2(k)$ at D is given as

$$y_2(k) = A\sqrt{P_0}h(k)s(k) + n(k) \tag{3}$$

where $h(k) = h_1(k)h_2(k)$ denotes the equivalent channel gain of the two-hop relay link, and $n(k) = Ah_2(k)n_1(k) + n_2(k)$ is the equivalent noise, where $n_2(k) \sim \mathcal{CN}(0, N_0)$ is the Gaussian noise at D.

In the aforementioned modeling, $h_i(k) \sim \mathcal{CN}(0, \sigma_i^2)$, $i = 0, 1, 2$ represent the complex channel gains of the S–D, S–R, and R–D channels at time index k, respectively. The channels are assumed to be mutually independent, and the AR(1) process is adopted to model the dynamics of each channel, i.e.,

$$h_i(k) = \alpha_i h_i(k-1) + \sqrt{1-\alpha_i^2}e_i(k) \tag{4}$$

where $\alpha_i = \mathcal{J}_0(2\pi f_i)$ is the normalized correlation coefficient of the channel h_i, $\mathcal{J}_0(\cdot)$ denotes the first-kind Bessel function of order zero, i.e., f_i is the normalized maximum Doppler frequency, and $e_i(k) \sim \mathcal{CN}(0, \sigma_i^2)$, which is independent of $h_i(k-1)$.

The average received signal-to-noise ratios (SNRs) per symbols γ_0 and γ_1 of the S–D and S–R links are respectively denoted by

$$\gamma_0 = \frac{P_0\sigma_0^2}{N_0} \qquad \gamma_1 = \frac{P_0\sigma_1^2}{N_0}. \tag{5}$$

According to (1) and (5), it is easy to show that $y_0(k) \sim \mathcal{CN}(0, N_0(1+\gamma_0)$. For a given $h_2(k)$, $n(k)$ and $y_2(k)$ can be characterized by conditional probability density functions (PDFs) $\mathcal{CN}(0, \sigma_n^2(k))$ and $\mathcal{CN}(0, \sigma_n^2(k)(1+\gamma_2(k)))$, where $\sigma_n^2(k) = N_0(1 + A^2|h_2(k)|^2)$, and $\gamma_2(k)$ is the equivalent SNR of the relay link, which is given by

$$\gamma_2(k) = \frac{A^2\gamma_1 |h_2(k)|^2}{1 + A^2 |h_2(k)|^2}. \tag{6}$$

III. Differential Maximum-Likelihood Combiner

Here, we propose a new DML combiner and derive a suboptimal weight for the DML combiner, which is more suitable for noncoherent systems.

We consider the employment of the maximum *a posteriori* detector to detect signals $y_0(k)$, $y_0(k-1)$, $y_2(k)$, and $y_2(k-1)$ at the destination. It follows from [21] that the detected symbol is computed according to the maximum log-likelihood rule as follows:

$$\hat{d}(k) = \arg\max_{d(k)\in S} \sum_{i\in\{0,2\}} \log\left(p\left(y_i(k)|y_i(k-1), d(k)\right)\right) \quad (7)$$

which utilizes the assumption that the transmitted symbols are equiprobable and the involved channels are independent. In addition, $p(\cdot|\cdot)$ represents the conditional PDF.

To compute $\hat{d}(k)$ in (7), the autocorrelation between the received signals from the direct and relay links during the two consecutive symbol periods is needed. It follows from (1)–(4) that:

$$E\left\{y_0(k)y_0^*(k-1)|d(k)\right\} = N_0\alpha_0\gamma_0 d(k) \quad (8)$$

$$E\left\{y_2(k)y_2^*(k-1)|h_2(k), h_2(k-1), d(k)\right\} = N_0\alpha_1 A^2\gamma_1 h_2(k)h_2^*(k-1)d(k). \quad (9)$$

Hence, for the given $y_0(k-1)$ and $d(k)$, $y_0(k)$ is a Gaussian random variable with conditional mean $\mu_0(k)$ and conditional variance Σ_0 [22], i.e.,

$$\mu_0(k) = \frac{E\left\{y_0(k)y_0^*(k-1)|d(k)\right\}}{\mathrm{Var}\left\{y_0(k-1)\right\}} y_0(k-1) = \frac{\alpha_0\gamma_0}{1+\gamma_0} y_0(k-1)d(k) \quad (10)$$

$$\Sigma_0 = \mathrm{Var}\left\{y_0(k)\right\} - \frac{\left|E\left\{y_0(k)(y_0^*(k-1)|d(k)\right\}\right|^2}{\mathrm{Var}\left\{y_0(k-1)\right\}} = N_0\left(1+\gamma_0 - \frac{\alpha_0^2\gamma_0^2}{\gamma_0+1}\right). \quad (11)$$

Moreover, for the given $y_2(k-1)$, $d(k)$, $h_2(k-1)$, and $h_2(k)$, $y_2(k)$ is also a Gaussian random variable with conditional mean $\mu_2(k)$ and conditional variance $\Sigma_2(k)$, i.e.,

$$\mu_2(k) = \frac{E\left\{y_2(k)y_2^*(k-1)|h_2(k), h_2(k-1), d(k)\right\}}{\mathrm{Var}\left\{y_2(k-1)\right\}} y_2(k-1) = \theta(k)y_2(k-1)d(k) \quad (12)$$

$$\Sigma_2(k) = \mathrm{Var}\left\{y_2(k)\right\} - \frac{\left|E\left\{y_2(k)y_2^*(k-1)|h_2(k), h_2(k-1), d(k)\right\}\right|^2}{\mathrm{Var}\left\{y_2(k-1)\right\}} = \sigma_n^2(k)\left(\gamma_2(k)+1\right) + \frac{\left|N_0\alpha_1 A^2\gamma_1 h_2(k)h_2^*(k-1)\right|^2}{\sigma_n^2(k-1)\left(\gamma_2(k-1)+1\right)} \quad (13)$$

where

$$\theta(k) = \frac{N_0\alpha_1 A^2\gamma_1 h_2(k)h_2^*(k-1)}{\sigma_n^2(k-1)\left(\gamma_2(k-1)+1\right)}. \quad (14)$$

By substituting the conditional PDFs of $y_0(k)$ and $y_2(k)$ into (7), we arrive at

$$\hat{d}(k) = \arg\max_{d(k)\in S}\left\{\log\left(\frac{e^{-\frac{|y_0(k)-\mu_0(k)|^2}{\Sigma_0}}}{\pi\Sigma_0}\right) + \log\left(\frac{e^{-\frac{|y_2-\mu_2(k)|^2}{\Sigma_2(k)}}}{\pi\Sigma_2(k)}\right)\right\}. \quad (15)$$

Substituting $\mu_0(k)$, Σ_0, $\mu_2(k)$, and $\Sigma_2(k)$ into (15) and dropping the irrelevant terms give rise to the following simplified decision metric:

$$\hat{d}(k) = \arg\max_{d(k)\in S}\left\{\mathrm{Re}\left\{w_0 y_0^*(k-1)y_0(k) + w_2^{\mathrm{opt}}(k)y_2^*(k-1)y_2(k)\right\}d(k)\right\} \quad (16)$$

where

$$w_0 = \frac{\alpha_0\frac{\gamma_0}{1+\gamma_0}}{\Sigma_0} = \frac{\alpha_0\gamma_0}{N_0\left((1+\gamma_0)^2 - \alpha_0^2\gamma_0^2\right)} \quad (17)$$

$$w_2^{\mathrm{opt}}(k) = \frac{\theta(k)}{\Sigma_2(k)} = \frac{A^2\alpha_1\gamma_1}{N_0 L(k)} \quad (18)$$

are the optimal combining weights with

$$L(k) = A^4\left((1+\gamma_1)^2 - \gamma_1^2\alpha_1^2\right)h_2(k)h_2^*(k-1) + \frac{A^2(1+\gamma_1)\left(|h_2(k)|^2 + |h_2(k-1)|^2\right)+1}{h_2(k)h_2^*(k-1)}. \quad (19)$$

The optimal weight w_2^{opt} is determined by the instantaneous CSI $h_2(k)$ and $h_2(k-1)$, which are unavailable at the destination. According to (18), one is able to obtain a time-independent version of w_2^{opt} by replacing all the $|h_2(k-1)|^2$ and $|h_2(k)|^2$ terms with the average σ_2^2 and all the $h_2(k)h_2^*(k-1)$ terms with $\alpha_2\sigma_2^2$ in $\theta(k)$ and $\Sigma_2(k)$, i.e.,

$$\tilde{\theta} = \frac{\alpha A^2\gamma_1\sigma_2^2}{1+A^2(1+\gamma_1)\sigma_2^2} \quad (20)$$

$$\tilde{\Sigma}_2 = N_0\left(1+A^2(1+\gamma_1)\sigma_2^2\right) - \frac{N_0\alpha^2A^4\gamma_1^2\sigma_2^4}{1+A^2(1+\gamma_1)\sigma_2^2} \quad (21)$$

where $\alpha = \alpha_1\alpha_2$ is the equivalent normalized correlation coefficient of the relay link.

By following a similar approach to (16), the suboptimal combining weight for the relay link can be derived as:

$$w_2 = \frac{\tilde{\theta}}{\tilde{\Sigma}} = \frac{\alpha A^2\gamma_1\sigma_2^2}{N_0\left(\left(1+A^2(1+\gamma_1)\sigma_2^2\right)^2 - A^4\alpha^2\gamma_1^2\sigma_2^4\right)}. \quad (22)$$

To gain more insights into the proposed suboptimal weights, the behavior of w_2/w_0 at the high-SNR region is analyzed. Dividing both the numerator and the denominator by P^4 and ignoring all the terms containing $1/P$, the term w_2/w_0 can be further simplified as follows:

$$\kappa = \lim_{P\to\infty}\frac{w_2}{w_0} = \frac{\alpha\left(1-\alpha_0^2\right)\sigma_0^4\sigma_1^4\sigma_2^2(1-\phi)\phi^3}{(1-\alpha^2)\alpha_0\sigma_0^2\sigma_1^4\sigma_2^4(1-\phi)^2\phi^2} = \frac{\alpha\left(1-\alpha_0^2\right)\sigma_0^2\phi + O\left(\frac{1}{P}\right)}{(1-\alpha^2)\alpha_0\sigma_2^2(1-\phi) + O\left(\frac{1}{P}\right)}. \quad (23)$$

It should be noted that the ratio of weight w_2 in (22) to w_0 in (17) is equal to that of the weights of the TVD scheme in [18] when the channel is symmetric.

IV. Universal BER Expression and Error Floor

Without loss of generality, we assume that the transmitted information symbol $d(k) = 1$. For given $h_2(k-1)$ and $h_2(k)$, the BER P_b can be expressed as

$$P_b(\varepsilon) = P\left\{\mathrm{Re}\left\{w_0 y_0^*(k-1)y_0(k) + w_2(k)y_2^*(k-1)y_2(k)\right\}\right\} < 0 = P\left\{|U_1|^2 + |U_2|^2 < |V_1|^2 + |V_2|^2 | d(k)=1, h_2(k), h_2(k-1)\right\} \quad (24)$$

where

$$\begin{aligned} U_1 &= \sqrt{w_0}\,(y_0(k-1) + y_0(k)) \\ U_2 &= \sqrt{w_2}\,(y_2(k-1) + y_2(k)) \\ V_1 &= \sqrt{w_0}\,(y_0(k-1) - y_0(k)) \\ V_2 &= \sqrt{w_2}\,(y_2(k-1) - y_2(k))\,. \end{aligned} \tag{25}$$

As aforementioned in Section II, U_1 and V_1 are both the sum of two Gaussian random variables. According to (8), we can obtain $E\{y_0(k) y_0^*(k-1)|d(k) = 1\} = \alpha_0 N_0 \gamma_0$. Then, we utilize the modified AR(1) model of the relay link proposed in [16], which is given as

$$h(k) = \alpha h(k-1) + \sqrt{1-\alpha^2} h_2(k-1) e_1(k). \tag{26}$$

Then, we have

$$E\{h(k)h^*(k-1)|d(k) = 1, h_2(k), h_2(k-1)\} = \alpha\sigma_1^2 \left|h_2(k-1)\right|^2. \tag{27}$$

Therefore, it follows that:

$$E\{y_2(k)y_2^*(k-1)|d(k) = 1, h_2(k-1)\} = \alpha\sigma_n^2(k-1)\gamma_2(k-1). \tag{28}$$

To further analyze the error performance of the proposed DML combiner, $\sigma_n^2(k)(1+\gamma_2(k))$ is approximated as $\sigma_n^2(k-1)(1+\gamma_2(k-1))$. This approximation has been widely used to analyze the error performance of D-AF systems over the time-selective channel ([16], [18], [23]) and has been proven to be extremely precise in [16].

Thus, the variances of the random variables in (25) are respectively given as follows [22]:

$$\begin{aligned} \sigma_{U_1}^2 &= 2w_0 N_0\,(1 + (1+\alpha_0)\gamma_0) \\ \sigma_{U_2}^2 &= 2w_2\sigma_n^2\,(1 + (1+\alpha)\gamma_2) \\ \sigma_{V_1}^2 &= 2w_0 N_0\,(1 + (1-\alpha_0)\gamma_0) \\ \sigma_{V_2}^2 &= 2w_2\sigma_n^2\,(1 + (1-\alpha)\gamma_2) \end{aligned} \tag{29}$$

in which the time index $(k-1)$ has been dropped for brevity. Hence, $|\psi|^2$, where $\psi \in \{U_1, U_2, V_1, V_2\}$, follows an exponential distribution, i.e.,

$$f_{|\psi|^2}(x) = \frac{1}{\sigma_\psi^2} e^{-\frac{x}{\sigma_\psi^2}}. \tag{30}$$

Let $C = |U_1|^2 + |U_2|^2$ and $D = |V_1|^2 + |V_2|^2$. Both C and D are hypoexponential random variables with two rate parameters $\{1/\sigma_{U_1}^2, 1/\sigma_{U_2}^2\}$ and $\{1/\sigma_{V_1}^2, 1/\sigma_{V_2}^2\}$, respectively. The PDFs of these two random variables can be shown as [24]

$$f_C(\zeta) = \frac{e^{-\frac{\zeta}{\sigma_{U_1}^2}} - e^{-\frac{\zeta}{\sigma_{U_2}^2}}}{\sigma_{U_1}^2 - \sigma_{U_2}^2} \tag{31}$$

$$f_D(\eta) = \frac{e^{-\frac{\eta}{\sigma_{V_1}^2}} - e^{-\frac{\eta}{\sigma_{V_2}^2}}}{\sigma_{V_1}^2 - \sigma_{V_2}^2}. \tag{32}$$

Hence, it follows that:

$$\begin{aligned} P_b(\varepsilon|h_2) &= P\{C < D|d(k) = 1, h_2\} \\ &= \int_0^\infty \int_0^\eta f_C(\zeta) f_D(\eta) d\zeta d\eta \\ &= 1 - \frac{\sigma_{U_1}^6}{\left(\sigma_{U_1}^2 - \sigma_{U_2}^2\right)\left(\sigma_{U_1}^2 + \sigma_{V_1}^2\right)\left(\sigma_{U_1}^2 + \sigma_{V_2}^2\right)} \\ &\quad + \frac{\sigma_{U_2}^6}{\left(\sigma_{U_1}^2 - \sigma_{U_2}^2\right)\left(\sigma_{U_2}^2 + \sigma_{V_1}^2\right)\left(\sigma_{U_2}^2 + \sigma_{V_2}^2\right)}. \end{aligned} \tag{33}$$

To attain the average BER, the conditional BER should be averaged over the distribution of $\lambda = |h2(k)|^2$. Therefore, after substituting (29) into (33) followed by some simplifications, the conditional BER can be transformed into:

$$\begin{aligned} P_b(\varepsilon|h_2) &= \frac{1+(1-\alpha)\gamma_1}{2(1+\gamma_1)} - \frac{K_1 w_2^2 \alpha^3 \gamma_1^3 \sigma_2^2}{2J_1 J_2 (1+\gamma_1)\left(\lambda + K_1\sigma_2^2\right)} \\ &\quad - \frac{w_0^2\left(1+(1+\alpha_0)\gamma_0\right)^3}{4A^2 J_2 w_2 (1+\gamma_0)\left(\lambda + K_2\sigma_2^2\right)} \\ &\quad + \frac{w_0^2\left(1+(1-\alpha_0)\gamma_0\right)^3}{4A^2 J_1 w_2 (1+\gamma_0)\left(\lambda + K_3\sigma_2^2\right)} \end{aligned} \tag{34}$$

where

$$\begin{aligned} J_1 &= -w_2\alpha\gamma_1 + w_0\left(1+(1-\alpha_0)\gamma_0\right)(1+\gamma_1) \\ J_2 &= w_2\alpha\gamma_1 + w_0\left(1+(1+\alpha_0)\gamma_0\right)(1+\gamma_1) \end{aligned}$$

$$K_1 = \frac{1}{A^2(1+\gamma_1)\sigma_2^2} \tag{35}$$

$$K_2 = \frac{w_2 + w_0\left(1+(1+\alpha_0)\gamma_0\right)}{A^2 w_2\left(1+(1-\alpha)\gamma_1\right)\sigma_2^2} \tag{36}$$

$$K_3 = \frac{w_2 + w_0\left(1+(1-\alpha_0)\gamma_0\right)}{A^2 w_2\left(1+(1+\alpha)\gamma_1\right)\sigma_2^2}. \tag{37}$$

Taking the expectation of (34) with respect to the exponential distribution of λ results in the following average BER:

$$\begin{aligned} P_b(\varepsilon) &= \frac{1+(1-\alpha)\gamma_1}{2(1+\gamma_1)} - \frac{e^{K_1} K_1 w_2^2 \alpha^3 \gamma_1^3 E_1(K_1)}{2J_1 J_2 (1+\gamma_1)} \\ &\quad - \frac{e^{K_2} w_0^2\left(1+(1+\alpha_0)\gamma_0\right)^3 E_1(K_2)}{4A^2 J_2 w_2 (1+\gamma_0)\sigma_2^2} \\ &\quad + \frac{e^{K_3} w_0^2\left(1+(1-\alpha_0)\gamma_0\right)^3 E_1(K_3)}{4A^2 J_1 w_2 (1+\gamma_0)\sigma_2^2}. \end{aligned} \tag{38}$$

It is noted that (38) is a universal average BER expression and can serve as a performance benchmark for diversity combiners with any weights w_0 and w_2 in D-AF systems. Equation (38) is exact but overly complex in terms of gains insights into the system error performance. To quantify the error floor of the proposed DML combiner, we first derive the relevant asymptotic error probability by setting the values of w_0 and w_2 according to (17) and (22). The details are explained as follows.

It follows from (35) that:

$$\tilde{K}_1 = \lim_{P\to\infty} K_1 = 0. \tag{39}$$

Then, using a similar method as in the derivation of $\lim_{P\to\infty} w_2/w_0$, we have

$$\tilde{K}_2 = \lim_{P\to\infty} K_2 = \frac{(1+\alpha)\alpha_0}{\alpha(1-\alpha_0)} \tag{40}$$

$$\tilde{K}_3 = \lim_{P\to\infty} K_3 = \frac{(1-\alpha)\alpha_0}{\alpha(1+\alpha_0)}. \tag{41}$$

The limit of the first term of P_b in (38) is given as

$$\lim_{P\to\infty} \frac{1+(1-\alpha)\gamma_1}{2(1+\gamma_1)} = \frac{1-\alpha}{2}. \tag{42}$$

Based on [25, eq. (6.8.2)], we have

$$\lim_{\tilde{K}_1\to 0} -\tilde{K}_1 e^{\tilde{K}_1} E_1(\tilde{K}_1) = 0. \tag{43}$$

Considering (22), it can be shown that

$$\lim_{P\to\infty} \frac{w_2^2\alpha^3\gamma_1^3}{2J_1 J_2 (1+\gamma_1)} = \frac{0 + O\left(\frac{1}{P}\right)}{2(1-\alpha^2)^2 \alpha_0^2 \sigma_0^4 \sigma_1^{10} \sigma_2^8 (1-\phi)^4 \phi^5 + O\left(\frac{1}{P}\right)} = 0. \tag{44}$$

TABLE I
OPTIMAL POWER ALLOCATION FACTORS

Channel scenarios	$(\sigma_0^2, \sigma_1^2, \sigma_2^2)$	ϕ_{opt}
symmetric channel	$(1, 1, 1)$	0.64
Better S-D channel	$(10, 1, 1)$	0.65
Better S-R channel	$(1, 10, 1)$	0.57

Hence, the limit of the second term of P_b in (38) is 0. With the aid of (17) and (22), it can be shown that

$$\lim_{P\to\infty} \frac{w_0^2\,(1+(1\alpha_0)\gamma_0)^3}{4A^2 J_2 w_2 (1+\gamma_0)\sigma_2^2} = \frac{(1-\alpha^2)\alpha_0(1+\alpha_0)+O\left(\frac{1}{P}\right)}{4\alpha(1-\alpha_0)+O\left(\frac{1}{P}\right)} = \frac{1}{4}\tilde{K}_2(1-\alpha)(1+\alpha_0). \quad (45)$$

Hence, the limit of the third term of P_b is derived as

$$-\frac{1}{4}e^{\tilde{K}_2}\tilde{K}_2(1-\alpha)(1+\alpha_0)E_1(\tilde{K}_2). \quad (46)$$

Similar to the derivation process of (44), it is easy to show that

$$\lim_{P\to\infty} \frac{\left(w_0^2\,(1+(1-\alpha_0)\gamma_0)^3\right)}{4A^2 J_1 w_2 (1+\gamma_0)\sigma_2^2} = \frac{(1-\alpha^2)(1-\alpha_0)\alpha_0+O\left(\frac{1}{P}\right)}{4\alpha(1+\alpha_0)+O\left(\frac{1}{P}\right)} = \frac{1}{4}\tilde{K}_3(1+\alpha)(1-\alpha_0). \quad (47)$$

Hence, the limit of the fourth term of P_b is given as

$$\frac{1}{4}e^{\tilde{K}_3}\tilde{K}_3(1+\alpha)(1-\alpha_0)E_1(\tilde{K}_3). \quad (48)$$

Therefore, the asymptotic error probability can be expressed as

$$\lim_{P\to\infty} P_b(\varepsilon) = \frac{1-\alpha}{2} - \frac{1}{4}e^{\tilde{K}_2}\tilde{K}_2(1-\alpha)(1+\alpha_0)E_1(\tilde{K}_2) + \frac{1}{4}e^{\tilde{K}_3}\tilde{K}_3(1+\alpha)(1-\alpha_0)E_1(\tilde{K}_3). \quad (49)$$

It can be inferred from (49) that an error floor occurs that is independent of the average channel quality of the involved channels, the total transmit power P, and the power-allocation ratio ϕ. The error floor only determined the autocorrelation of the direct and relay links.

V. NUMERICAL RESULTS

Here, numerical results are presented to verify the analyses derived in Sections III and IV. Three scenarios of the average channel gain are considered: 1) a symmetric channel with all channel variances $\sigma_0^2 = \sigma_1^2 = \sigma_2^2 = 1$; 2) an asymmetric channel with a better average S–D channel quality, i.e., $\sigma_0^2 = 10$, $\sigma_1^2 = \sigma_2^2 = 1$; and 3) an asymmetric channel with a better average S–R channel quality, i.e., $\sigma_0^2 = \sigma_2^2 = 1$, $\sigma_1^2 = 10$. The simulation model in [26] is used to generate the channel coefficients. Similar to [16], three fading scenarios are considered as follows: I) all the channels undergo slow fading with $f_0 = f_1 = f_2 = 0.001$; II) the S–R and S–D channels are fast fading with $f_0 = f_1 = 0.02$, whereas the R–D channel undergoes slow fading with $f_2 = 0.001$; and III) all the channels are fast fading with $f_0 = 0.05$, $f_1 = 0.01$, and $f_2 = 0.04$.

Assuming that all the channels are slow fading, Table I shows the optimal power allocation factor ϕ_{opt} for the DML combiner, which are obtained numerically by minimizing the BER in (38) at $P/N_0 = 25$ dB.

Fig. 2 plots κ and the ratio of the weights of CDD scheme (i.e., κ_0) by using optimal power allocation versus P/N_0 under the three fading scenarios and the symmetric channel configuration. With the increase of P/N_0, κ becomes significantly larger than κ_0 at 25 and 30 dB in

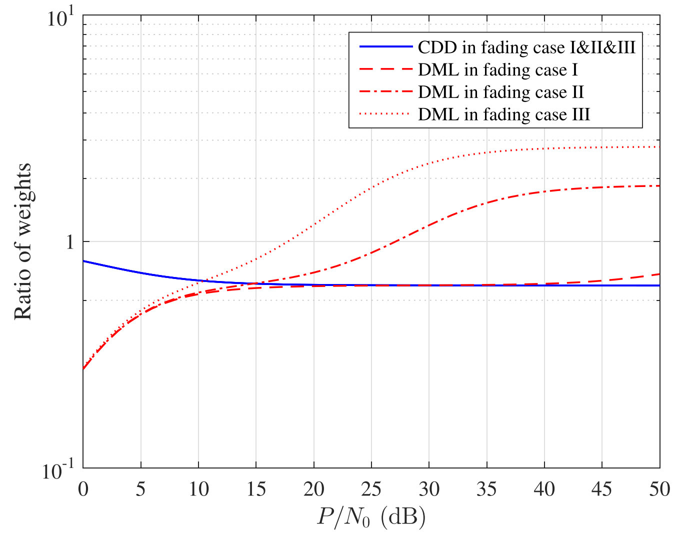

Fig. 2. Ratio of the weights of the DML and CDD combiners as a function of P/N_0 under the three fading scenarios and the symmetric channel configuration.

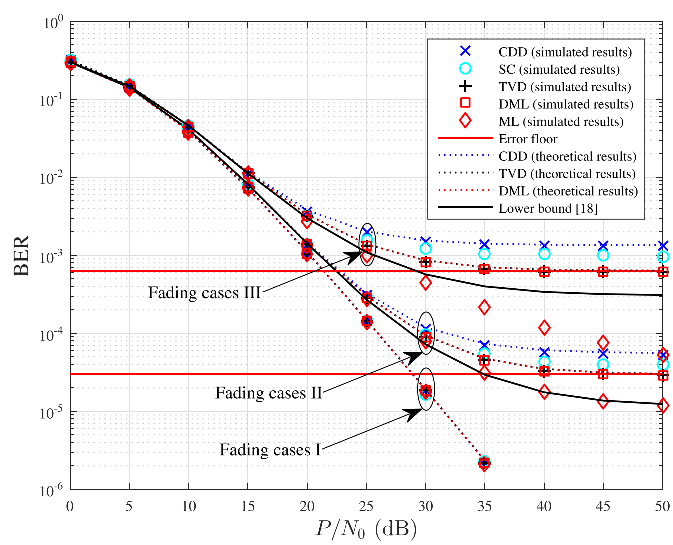

Fig. 3. BER comparison of the CDD, SC, DML, and TVD schemes in the symmetric channel with $\sigma_0^2 = \sigma_1^2 = \sigma_2^2 = 1$.

fading scenarios II and III, respectively. In fading scenario I, the difference between κ and κ_0 is negligible. Intuitively, when all the channels fade slowly, the autocorrelation of the S–D channel and the relay channel has a minimal impact on the computation of w_0 and w_2. By contrast, when the links become fast fading, the channel with the larger autocorrelation will be more influential in the decision metric in (16).

Figs. 3–5 aim to verify the accuracy of the universal average BER expression in (38) with the CDD and DML schemes under the given fading scenarios with a range of average channel qualities. Note that the TVD scheme proposed in [18] for the symmetric channel is also plotted in Fig. 3. Moreover, the simulation results of the SC scheme proposed in [16] are also plotted for comparative purposes. It is clearly shown that, for all the fading scenarios, the approximate theoretical BER expressions match well with the simulated BER curves of the first three schemes. Hence, (38) can be used to benchmark the error performance of diversity combining algorithms, which utilize all the received signals in the D-AF system over the time-selective channel.

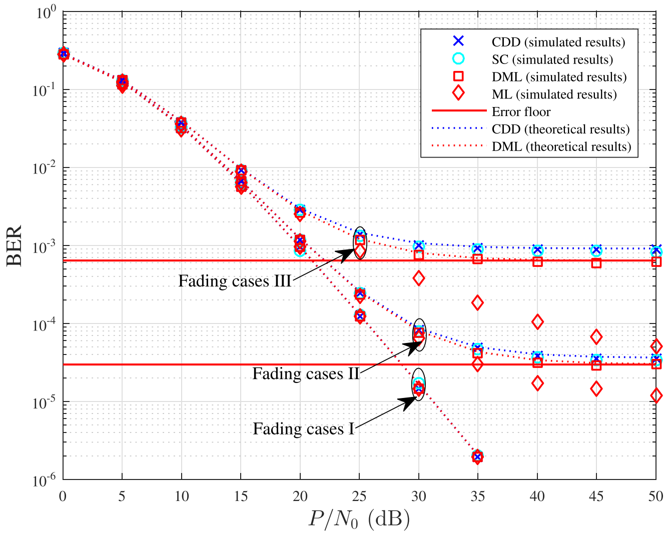

Fig. 4. BER comparison of the CDD, SC, and DML schemes in the asymmetric channel with $\sigma_0^2 = \sigma_2^2 = 1$ and $\sigma_1^2 = 10$.

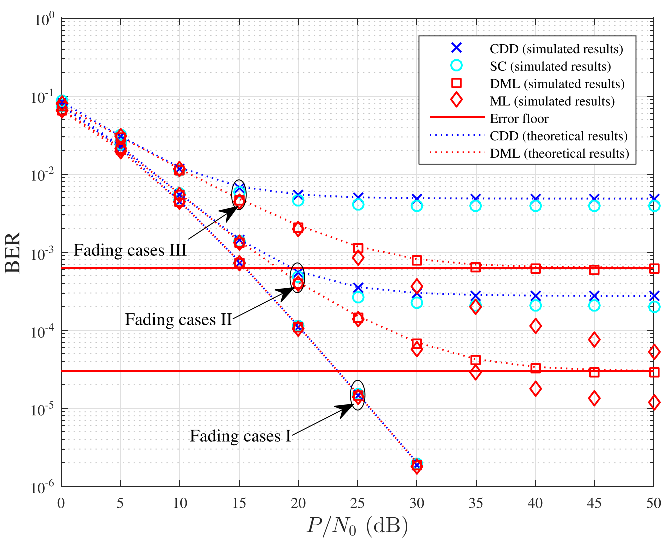

Fig. 5. BER comparison of the CDD, SC, and DML schemes in the asymmetric channel with $\sigma_0^2 = 10$ and $\sigma_1^2 = \sigma_2^2 = 1$.

As can be observed in Fig. 3, the proposed DML scheme and the TVD scheme have the same error performance over the entire region of P/N_0 in all the fading scenarios. For fading scenario I, the performances of the TVD, CDD, and DML algorithms are identical to that of the ML scheme, which do not exhibit an error floor. Meanwhile, in fading scenarios II and III, we can achieve the following results. First, all the schemes yield almost the same performance when P/N_0 is low, and the performance gap becomes larger with the increase of P/N_0. Second, the ML scheme demonstrates the best performance for both fading scenarios II and III, provided that the instantaneous CSI is known at the receiver. However, this assumption is almost impossible for the D-AF system. It is noted that the performance of the ML combiner is better than the lower bound proposed in [18] for fading case III, whereas the two are the same for fading cases I and II.

As shown in Figs. 3–5, all the schemes perform the best in fading scenario I with the average channel qualities specified in Fig. 5. However, the opposite is true when any link becomes time selective, and all the schemes incur more serious performance degradation than in the other channel variance scenarios. However, the DML

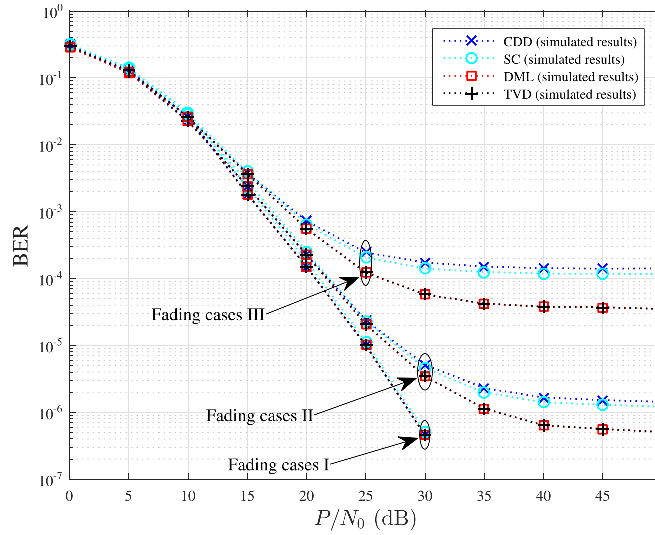

Fig. 6. BER comparison of the CDD, SC, DML, and TVD schemes with two relays in the symmetric channel.

scheme can keep the same error floor for both fading scenarios II and III. According to (4), the absolute difference between two consecutive received symbols is proportional to both the normalized correlation coefficient and the channel variance. In other words, when the normalized correlation coefficient remains unchanged, the channel with a larger variance results in more severe performance degradation. When the average channel quality of the S–D link is better than that of the other two links, the DML scheme can reduce the influence of the S–D link in the decision metric in (16), to mitigate the impact of the time selectivity on the system performance.

As the number of the relays increases, the theoretical BER analysis of D-AF system that uses the linear combiner becomes intractable. Fig. 6 plots the numerical results of the D-AF system with two relays employing the CDD, SC, TVD, and DML schemes for the symmetric channel scenario. As shown in the figure, all the schemes achieve better performance than in the single-relay scenario.

VI. Conclusion

This paper has studied the error performance of the single-relay D-AF system considering BPSK signaling over a time-selective fading channel. A differential diversity combiner was proposed, which can weigh the received signals of the direct and relay links based on the average channel quality and correlation coefficient. Moreover, a universal approximate expression for the average BER of the proposed scheme was derived. In addition, an asymptotic BER expression was provided to analyze the proposed scheme. The impact of a variety of Doppler frequencies and average channel gains on the system performance was further investigated. It was observed that, for the fast-fading scenarios, the error performance of the system is determined by both the average channel gain and the fading rate of each channel involved at the low-SNR region. However, at the high-SNR region, an error floor is exhibited that is only determined by the fading rates. Both theoretical and simulated results were presented to show that the proposed scheme outperforms the CDD and SC schemes.

References

[1] M. Dohler and Y. H. Li, *Cooperative Communications: Hardware, Channel & PHY*. Hoboken, NJ, USA: Wiley, 2010.

[2] F. Boccardi, R. W. Heath, A. Lozano, T. L. Marzetta, and P. Popovski, “Five disruptive technology directions for 5G,” *IEEE Commun. Mag.*, vol. 52, no. 2, pp. 74–80, Feb. 2014.

[3] J. Y. Zhang, L. L. Yang, L. Hanzo, and H. Gharavi, "Advances in cooperative single-carrier FDMA communications: Beyond LTE-Advanced," *IEEE Commun. Surveys Tuts.*, vol. 17, no. 2, pp. 730–756, May 2015.

[4] J. G. Andrews *et al.*, "What will 5G be?" *IEEE J. Sel. Areas Commun.*, vol. 32, no. 6, pp. 1065–1082, Jun. 2014.

[5] J. N. Laneman, D. N. C. Tse, and G. W. Wornell, "Cooperative diversity in wireless networks: Efficient protocols and outage behavior," *IEEE Trans. Inf. Theory*, vol. 50, no. 12, pp. 3062–3080, Dec. 2004.

[6] G. J. Chen, Z. Tian, Y. Gong, Z. Chen, and J. A. Chambers, "Max-ratio relay selection in secure buffer-aided cooperative wireless networks," *IEEE Trans. Inf. Forensics Security*, vol. 9, no. 4, pp. 719–729, Apr. 2014.

[7] D. S. Michalopoulos, H. A. Suraweera, G. K. Karagiannidis, and R. Schober, "Amplify-and-forward relay selection with outdated channel estimates," *IEEE Trans. Commun.*, vol. 60, no. 5, pp. 1278–1290, May 2012.

[8] M. Soysa, H. A. Suraweera, C. Tellambura, and H. K. Garg, "Partial and opportunistic relay selection with outdated channel estimates," *IEEE Trans. Commun.*, vol. 60, no. 3, pp. 840–850, May 2012.

[9] J. M. Moualeu, W. Hamouda, and F. Takawira, "Relay selection for coded cooperative networks with outdated CSI over Nakagami-m fading channels," *IEEE Trans. Wireless Commun.*, vol. 13, no. 5, pp. 2362–2373, May 2014.

[10] H. Y. Song, L. Song, and B. L. Jiao, "Weighted bidirectional relay selection for outdated channel state information," *IEEE Trans. Commun.*, vol. 62, no. 2, pp. 500–509, Feb. 2014.

[11] Y. Khattabi and M. M. Matalgah, "Performance analysis of AF cooperative networks with time-varying links: Error rate and capacity," in *Proc. WTS*, Washington, DC, USA, 2014, pp. 1–6.

[12] Y. Khattabi and M. M. Matalgah, "Performance analysis of multiple-relay AF cooperative systems over Rayleigh time-selective fading channels with imperfect channel estimation," *IEEE Trans. Veh. Technol.*, vol. 65, no. 1, pp. 427–434, Jan. 2016.

[13] Q. Zhao and H. B. Li, "Performance of differential modulation with wireless relays in Rayleigh fading channels," *IEEE Commun. Lett.*, vol. 9, no. 4, pp. 343–345, Apr. 2005.

[14] T. Himsoon, W. F. Su, and K. J. R. Liu, "Differential transmission for amplify-and-forward cooperative communications," *IEEE Signal Process. Lett.*, vol. 12, no. 9, pp. 597–600, Sep. 2005.

[15] Q. Zhao and H. B. Li, "Differential modulation for cooperative wireless systems," *IEEE Trans. Signal Process.*, vol. 55, no. 5, pp. 2273–2283, May 2007.

[16] M. R. Avendi and H. H. Nguyen, "Performance of selection combining for differential amplify-and-forward relaying over time-varying channels," *IEEE Trans. Wireless Commun.*, vol. 13, no. 8, pp. 4156–4166, Aug. 2014.

[17] J. G. Proakis and M. Salehi, *Digital Communications*. New York, NY, USA: McGraw-Hill, 2008.

[18] M. R. Avendi and H. H. Nguyen, "Performance of differential amplify-and-forward relaying in multinode wireless communications," *IEEE Trans. Veh. Technol.*, vol. 62, no. 8, pp. 3603–3613, Oct. 2013.

[19] P. Y. Kam, "Bit error probabilities of MDPSK over the nonselective Rayleigh fading channel with diversity reception," *IEEE Trans. Commun.*, vol. 39, no. 2, pp. 220–224, Feb. 1991.

[20] F. Adachi, "Postdetection optimal diversity combiner for DPSK differential detection," *IEEE Trans. Veh. Technol.*, vol. 42, no. 3, pp. 326–337, Aug. 1993.

[21] H. Fu and P. Y. Kam, "Performance of optimum and suboptimum combining diversity reception for binary and quadrature DPSK over independent, nonidentical Rayleigh fading channels," *IEEE Trans. Commun.*, vol. 55, no. 5, pp. 887–894, May 2007.

[22] A. Papoulis and S. U. Pillai, *Probability, Random Variables, and Stochastic Processes*, 4th ed. New York, NY, USA: McGraw-Hill, 2002.

[23] M. R. Avendi and H. H. Nguyen, "Differential dual-hop relaying under user mobility," *IET Commun.*, vol. 8, no. 17, pp. 3161–3169, Nov. 2014.

[24] S. M. Ross, *Introduction to Probability Models*. New York, NY, USA: Academic, 2014.

[25] F. W. J. Olver, D. W. Lozier, R. F. Boisvert, and C. W. Clark, *NIST Handbook of Mathematical Functions*. New York, NY, USA: Cambridge Univ. Press, 2010.

[26] Y. H. R. Zheng and C. S. Xiao, "Improved models for the generation of multiple uncorrelated Rayleigh fading waveforms," *IEEE Commun. Lett.*, vol. 6, no. 6, pp. 256–258, Jun. 2002.

Constructive Interference as an Information Carrier by Dual-Layered MIMO Transmission

Christos Masouros, *Senior Member, IEEE*, and Lajos Hanzo, *Fellow, IEEE*

***Abstract*—We propose a bandwidth-efficient transmission scheme for multiple-input–multiple-output point-to-point and downlink channels. The bandwidth efficiency (BE) of spatial multiplexing (SMX) is improved by implicitly encoding information in the spatial domain based on the existence of constructive interference in the received symbols, which creates a differentiation in the symbol power. Explicitly, the combination of symbols received at a higher power level carries implicit information in the spatial domain in the same manner as that the combination of nonzero elements in the received symbol vector carries information for receive-antenna-based spatial modulation (RSM). The nonzero power throughout the received symbol vector for the proposed technique allows a full SMX underlying transmission, with the BE enhancement brought by the spatial symbol. Our simulation results demonstrate both significant BE gains and error probability reduction for our approach over the conventional SMX and RSM schemes.**

***Index Terms*—Multiple-input multiple-output (MIMO), precoding, spatial modulation (RSM), spatial multiplexing (SMX).**

I. Introduction

Multiple-input multiple-output (MIMO) systems have been shown to improve the capacity of the wireless channel by means of spatial multiplexing (SMX). Transmit precoding (TPC) schemes introduced for multiuser downlink (DL) transmission improve both the power efficiency and cost of mobile stations by shifting the signal processing complexity to the base stations. From the wide range of linear and nonlinear TPC schemes found in the literature, here, we focus our attention on the family of closed-form linear TPC schemes based on channel inversion [1], [2], which pose low computational complexity. More recently, spatial modulation (SM) has been explored as a means of implicitly encoding information in the index of the specific transmit antenna (TA) activated for the transmission of the modulated symbols, which offers a low-complexity design alternative [3]. Its central benefits include the absence of interantenna interference and the fact that, in contrast to SMX, it only requires a subset (down to one) of radio-frequency chains compared with SMX. Early work has focused on the design of receiver algorithms for minimizing the bit error ratio (BER) of SM at low complexity [3]–[5].

In addition to receive processing, recent work has also proposed constellation shaping for SM [6]–[14]. Specifically, the contributions on this topic have focused on three main directions: 1) shaping and optimization of the spatial constellation, i.e., the legitimate sets of activated TAs [6]; 2) modulation constellation shaping [7]–[9] for the

Manuscript received June 20, 2015; revised November 3, 2015; accepted February 8, 2016. Date of publication April 27, 2016; date of current version December 14, 2016. This work was supported in part by the U.K. Royal Academy of Engineering and in part by the Engineering and Physical Sciences Research Council through Project EP/M014150/1. The review of this paper was coordinated by Prof. W. A. Krzymień.

C. Masouros is with the Department of Electrical & Electronic Engineering, University College London, London WC1E 7JE, U.K. (e-mail: chris.masouros@ieee.org).

L. Hanzo is with the School of Electronics and Computer Science, University of Southampton, Southampton SO17 1BJ, U.K. (e-mail: lh@ecs.soton.ac.uk).

Color versions of one or more of the figures in this paper are available online at http://ieeexplore.ieee.org.

Digital Object Identifier 10.1109/TVT.2016.2528506